VERSITA

DOI: 10.2478/v10299-012-0010-5

An Energetic Approach for Numerical Analysis of an Interface crack in Shearing Mode

Roman Vodička

Technical University of Košice
Civil Engineering Faculty, Institute of Construction Technology and Management
e-mail: roman.vodicka@tuke.sk

Abstract

A mathematical model of a layered structure and initiation and growth of interface cracks are presented. A numerical approach for solving this problem is described, with the emphasis to the analysis of a shearing-mode crack. The model defines a scalar damage variable in the interface and also plastic tangential slip, which increases the fracture toughness in the shearing crack mode. An energetic formulation governing the adhesive damage until it breaks is proposed. The approach is also tested numerically to demonstrate the behaviour of the model and to assess its suitability in a particular physical situation.

Key words: interface crack, interface plasticity, energetic approach, quadratic programming

1 Introduction

Number of applications of layered structures is increasing in recent years. Therefore, solving the problems with such structures and proposing mathematical models for them seems to be very important. In many situations the interface between layers, usually represented by a relatively thin adhesive layer, can be partially or fully damaged such process is frequently referred to as delamination or debonding of material layers. In this work, a numerical approach for solving delamination problems is discussed. The approach is, however, more general and it can be applied also to other situations where damage appears along an interface.

The initiation and growth of a crack appearing in an interface depends on the applied load and usually is motivated by Griffith theory [1]. The simplified version of the interface rupture does not distinguish energetically between the opening mode (Mode I) and shearing mode (Mode II). Observations of experimental results, however, prove that considerably more energy is usually needed to perform delamination in shearing mode, see [2],[3],[4],[5]. The sensitivity of the crack to its mode and its evolution is in engineering practice usually considered as directly dependent on the so-called fracture mode mixity angle as e.g. in [6][7].

Another approach, based on the microscopic analysis of interface rupture and its plastic response, see [4][5], determines two interface variables. First, a damage parameter of classical damage mechanics [8] describes the level of deterioration of the interface adhesive [9]. Second, a kind of plastic deformation controls a slip that may occur in the interface tangent direction before the adjacent bulk layers debond as discussed in [10],[11].

A rigorous mathematical solution is obtained by variational methods [12]. Numerical algorithms frequently have to cope with non-convex character of the energy functional [9][13][14][15]. Nevertheless, their restrictions to some of the unknown parameters are even quadratic [9], so that quadratic programming methods [16] are applicable.

In the present work the approach based on [10] is used. The analysis is focused on the behaviour of the interface adhesive in shearing mode, where both of the aforementioned interface parameters are active. The model is described in Section 2: the general case in Section 2.1, and a special case in which the effect of bulk domains is neglected in Section 2.2. The numerical analysis is focused on this special case and includes algorithms for minimizing of energy functional by effective conjugate gradient schemes. Some details of the computer implementation are shown in Section 3 and also in Appendix. The special case of the proposed approach is tested numerically in Section 4.

2 A model of interface failure

Let us consider a body defined by a planar domain $\Omega \subset R^2$ with a bounded Lipschitz boundary $\partial\Omega = \Gamma$. Let **n** denote the unit outward normal vector defined at the smooth part of Γ. A split into two non-overlapping subdomains Ω^A and Ω^B whose respective boundaries are Γ^η η=A,B, will be considered hereinafter for the sake of simplicity, Figure 1.

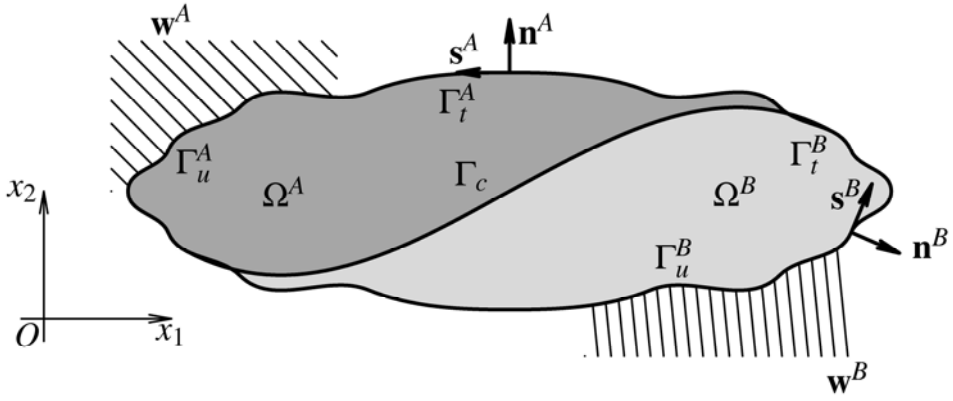

Figure 1: Model for an interface crack between two subdomains.

The common part of Γ^η called interface is denoted as Γ_c. The boundary conditions prescribed on a part of the outer boundary represent a hard-device loading, i.e. prescribed displacements $\mathbf{u}^\eta=\mathbf{w}^\eta$ over Γ_u^η. The remaining parts of the outer boundaries, denoted as Γ_t^η, are traction free, i.e. prescribed tractions $\mathbf{t}^\eta=\mathbf{0}$.

The interface Γ_c is considered as a very thin adhesive layer represented by a continuous spring distribution with normal and tangential elastic stiffnesses k_n and k_t, respectively. It is considered that a crack can appear along the interface Γ_c, this debonding process being considered as rate-independent. During this process, the material of the adhesive layer is damaged. This is modelled by a scalar damage variable ζ which varies at each interface point between one and zero [8]: values one and zero, respectively, corresponding to undamaged and fully damaged adhesive at a particular point. In addition to this variable, a plastic tangential slip variable π is considered at the interface. It allows for a difference between crack opening mode and shearing mode in view of experimental observations of interface crack growth. The observations confirm the energy dissipated in shearing mode to be significantly greater than that dissipated in opening mode and also correspondingly the associated plastic zones in the adjacent bulk to be larger in shearing mode than in opening mode. Thus some additional dissipated energy is considered for interface fracture in mode II as a useful and practical approximation of the plastic phenomena appearing in relatively narrow plastic zones in the bulk located in the interface vicinity, see [5][4].

2.1 Governing relations

Let us consider the energy stored at time τ in the structure obeying the aforementioned type of interface damage and a kinematic-hardening-plasticity model [10], with the plastic slope k_{H}, as

$$E(\tau,\mathbf{u},\zeta,\pi)=\sum_{\eta=A,B}\left[\int_{\Omega^\eta}\tfrac{1}{2}C^\eta_{ijkl}\varepsilon_{ij}\left(\mathbf{u}^\eta\right)\varepsilon_{kl}\left(\mathbf{u}^\eta\right)\mathrm{d}\Omega\right.$$
$$\left.+\int_{\Gamma_c}\left(\zeta\left(\tfrac{1}{2}k_n\left[\mathbf{u}\right]_n^2+\tfrac{1}{2}k_t\left(\left[\mathbf{u}\right]_t-\pi\right)^2\right)+\tfrac{1}{2}k_{\mathrm{H}}\pi^2+\tfrac{1}{2}k_0\left(\tfrac{\partial\zeta}{\partial s}\right)^2\right)\mathrm{d}\Gamma\right]. \tag{1}$$

It is valid for the state variables satisfying the boundary conditions on Γ_u^η and the condition of Signorini unilateral contact $\left[\mathbf{u}\right]_n\geq 0$ on Γ_c, where the relative normal displacement $\left[\mathbf{u}\right]_n=\left(\mathbf{u}^{\mathbf{A}}-\mathbf{u}^{\mathbf{B}}\right)\cdot\mathbf{n}^{\mathbf{A}}$ is introduced. Similarly, the relative tangential displacement $\left[\mathbf{u}\right]_t$ is defined. Next, the damage variable ζ should satisfy the constraints $0\leq\zeta\leq 1$. Otherwise, as a physically non-achievable state, the energy is assigned infinity. Here also, C_{ijkl} is the fourth-order tensor of elastic stiffness and ε_{ij} is small strain tensor pertinent to the bulk displacements $\mathbf{u}$. The last boundary term contains the tangential derivative of the damage $\frac{\partial\zeta}{\partial s}$ ($\mathbf{s}$ being a unit tangential vector, see Figure 1) and an auxiliary parameter k_0. The term is included for facilitating the mathematical treatment and for making the damage formulation non-local. It is usual in the gradient theory for internal parameters, see [17].

The dissipation potential for a rate independent process can be represented by a degree 1 homogeneous functional of the rates of pertinent variables, in our case the interface damage $\dot{\zeta}=\frac{\partial\zeta}{\partial\tau}$ and the plastic slip $\dot{\pi}=\frac{\partial\pi}{\partial\tau}$. The interface dissipation potential is given as follows:

$$R\left(\dot{\zeta},\dot{\pi}\right)=\int_{\Gamma_c}\left(G_d\left|\dot{\zeta}\right|+\sigma_{\mathrm{yield}}\left|\dot{\pi}\right|\right)\mathrm{d}\Gamma \tag{2}$$

The parameter G_d is the (minimum) interface fracture energy required to make a unit interface crack following the linear elastic-brittle part of the interface constitutive law. The initiation of the plastic slip is triggered when the interface yield shear stress σ_{yield} is achieved.

The solution evolution is governed by the following system of nonlinear variational inclusions

$$\begin{aligned} \partial_{\mathbf{u}} E(\tau,\mathbf{u},\zeta,\pi) \ni 0, \\ \partial_{\dot{\zeta}} R(\dot{\zeta},\dot{\pi}) + \partial_{\zeta} E(\tau,\mathbf{u},\zeta,\pi) \ni 0, \\ \partial_{\dot{\pi}} R(\dot{\zeta},\dot{\pi}) + \partial_{\pi} E(\tau,\mathbf{u},\zeta,\pi) \ni 0, \end{aligned} \tag{3}$$

where the symbol ∂ refers to partial subdifferential relying on convexity of pertinent functionals with respect to each particular variable, see [13].

The solution of nonlinear inclusions in engineering practice can be replaced by a form of a weak solution called energetic solution which was developed, for example, in [14]. Such a form of the solution is easier understandable for engineers, see [10][11], and also provides, from mathematical point of view, a concept which enables a generalization of convex optimization to the case of non-convex energies which unfortunately occurs in our model.

The energetic solution to the rate-independent problem (3) is a process $(\mathbf{u}(\tau),\zeta(\tau),\pi(\tau))$, $\tau \in [0;T]$, for which the following three conditions are satisfied:

- *Initial conditions*:

$$\mathbf{u}(0) = \mathbf{u}_0, \quad \zeta(0) = \zeta_0, \quad \pi(0) = \pi. \tag{4}$$

- *Stability inequality*: For any appropriate $(\tilde{\mathbf{u}},\tilde{\zeta},\tilde{\pi})$ it holds

$$E(\tau,\mathbf{u}(\tau),\zeta(\tau),\pi(\tau)) \le E(\tau,\tilde{\mathbf{u}},\tilde{\zeta},\tilde{\pi}) + R(\tilde{\zeta}-\zeta(\tau),\tilde{\pi}-\pi(\tau)) \tag{5}$$

- *Energy equality:*

$$E(\tau,\mathbf{u}(\tau),\zeta(\tau),\pi(\tau)) + \int_0^T R(\dot{\zeta}(\tau),\dot{\pi}(\tau))\,\mathrm{d}\tau = \int_0^T \partial_t E(\tau,\mathbf{u}(\tau),\zeta(\tau),\pi(\tau))\,\mathrm{d}\tau + E(\tau,\mathbf{u}_0,\zeta_0,\pi_0). \tag{6}$$

The stability condition (5) is a derivative free expression for finding the (global) minimum of energy functionals. The equation (6) provides an energetic balance of the stored energy, the dissipated energy and the work done by the external forces.

2.2 Model simplification for rupture by shearing slip

The present formulation can be simplified to test its behaviour in a numerical solution for the case of purely tangential loading resulting in a shearing crack. To do this, the influence of bulk regions is eliminated by considering the adjacent bulks rigid. The simplification, of course, removes the dependence of the crack evolution on the bulk material properties. Additionally, the upper body is considered to slip horizontally, with prescribed displacements obeying the rules $[\![\mathbf{u}]\!]_n = 0$ and $[\![\mathbf{u}]\!]_t = v(\tau)$ as it is also sketched in Figure 2. The function $v(\tau)$

is in fact a function of x_1, normally a constant function for the rigid bulk. Nevertheless, it can be prescribed by a slightly changing function in order the imperfections to take into account, e.g. changing of the adhesive thickness or of the bulk shapes.

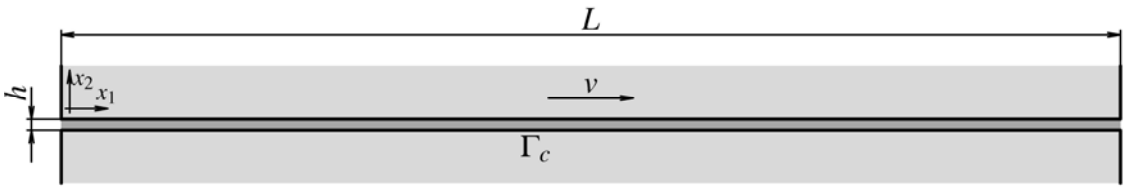

Figure 2: Geometry for the model with shearing slip

The stored energy $\mathcal{E}$ from (1) then reduces to

$$E_{\mathrm{S}}(\tau,\zeta,\pi)=\int_{\Gamma_c}\left(\tfrac{1}{2}\zeta k_t\left(v(\tau)-\pi\right)^2+\tfrac{1}{2}k_{\mathrm{H}}\pi^2+\tfrac{1}{2}k_0\left(\tfrac{\partial\zeta}{\partial s}\right)^2\right)\mathrm{d}\Gamma\Big]. \tag{7}$$

The unknowns remain only along the interface.

3 Notes on the numerical implementation of the model

A numerical approach to obtain the above defined energetic solution usually considers time and spatial discretizations separately. The time discretization provides the solution at time-steps defined by an increment δ such that $\tau_\lambda=\lambda\delta$ for $\lambda=1,2,\ldots,T/\delta$. The time-stepping procedure starts with the solution for $\lambda=1$ calculated from the initial conditions (4).

The stability condition (5) provides the minimization problem for the solution at the successive step λ, once the solution for the time step $\lambda-1$ is known, c. f. [10],

$$\text{minimize } H^{\lambda}(\zeta,\pi)=E_{\mathrm{S}}(\lambda\delta,\zeta,\pi)+R\left(\zeta-\zeta^{\lambda-1},\pi-\pi^{\lambda-1}\right) \tag{8}$$

Unfortunately, functional $\mathcal{H}^{\lambda}$ is not convex. Its non-convexity requires applying a special numerical treatment in a minimization algorithm. The alternative minimization algorithm (AMA) proposed in [15] has been used to split the minimization to alternation between minimization with respect to π and with respect to ζ, each of these being a minimization of a convex functional. The scheme of AMA written in MATLAB [18] can be seen in Appendix, Table 1.

The absolute values in $\mathcal{R}$, see (2) and (8), can hopefully be eliminated. The first one with ζ does not cause problem as long as it must be non-increasing, thus only $\zeta\leq\zeta^{\lambda-1}$ is admitted. For the second term, a classical trick of removing the absolute values and replacing them by additional unknowns with restrictions is used, see e.g. [19]. The solution of the original

problem (8) with $\mathcal{R}(\zeta\text{-}\zeta^{\lambda\text{-}1},\pi\text{-}\pi^{\lambda\text{-}1})$ is then the same as the solution with $\mathcal{R}(\zeta\text{-}\zeta^{\lambda\text{-}1},\omega)$ and a couple of the following additional constraints:

$$\begin{aligned}\omega-\pi &\geq -\pi^{\lambda-1}\\ \omega+\pi &\geq \pi^{\lambda-1}\end{aligned} \tag{9}$$

The alternation by AMA, however, does not have to lead to global minimization which is the characteristic of the energetic solution. Therefore a back-tracking algorithm (BTA) to control the process has been utilized, providing that the energy equality (6), in discrete form converted to a two-sided inequality is satisfied, see [9]. The two-sided inequality can be written in the following form to compare the energies in two subsequent time steps:

$$\begin{aligned}&\int_{\delta(\lambda-1)}^{\delta\lambda}\partial_\tau E\left(\tau,\mathbf{u}^{\lambda},\zeta^{\lambda},\pi^{\lambda}\right)\mathrm{d}\tau\\ &\quad\leq E\left(\delta\lambda,\mathbf{u}^{\lambda},\zeta^{\lambda},\pi^{\lambda}\right)-E\left(\delta(\lambda-1),\mathbf{u}^{\lambda-1},\zeta^{\lambda-1},\pi^{\lambda-1}\right)+R\left(\zeta^{\lambda}-\zeta^{\lambda-1},\pi^{\lambda}-\pi^{\lambda-1}\right)\\ &\qquad\leq\int_{\delta(\lambda-1)}^{\delta\lambda}\partial_\tau E\left(\tau,\mathbf{u}^{\lambda-1},\zeta^{\lambda-1},\pi^{\lambda-1}\right)\mathrm{d}\tau.\end{aligned} \tag{10}$$

Although, there is no guarantee that the process converges to the global minimum, the practical experience with BTA, however, shows that it provides a solution with lower energy than that obtained by mere AMA. The scheme of BTA written in MATLAB can be seen in Appendix, Table 2.

A conjugate gradient based algorithm with constraints, see [16], can be used in the minimization procedure with respect to either unknown as the pertinent energies are quadratic. A particular implementation of Polyak algorithm is sketched in Appendix, Table 3.

4 An example

The simplified case described in Section 2.2 is considered for the numerical simulation. The unknowns for each load step λ remain only along the interface (damage ζ^{λ}, plastic slip π^{λ}) and the displacement $v(\lambda\delta)=v_\lambda$ is prescribed as

$$\mathrm{v}_\lambda\left(x_1\right)=\sin\tfrac{\lambda\pi}{50}\left(1+5\sin\left(\pi x_1\right)\right)\cdot 0.002\mathrm{mm}. \tag{11}$$

The length of the glued faces of the bulks is l=1000mm. The adhesive material is epoxy resin, with elastic properties $E=2.4\times10^3$MPa and ν=0.33. Considering the adhesive layer thickness h=0.2mm, the corresponding stiffness parameter is $k_t=4.5\times10^3\mathrm{MPamm}^{-1}$, the details of the parameter statement can be seen e.g. in [20].

The parameters that govern the crack growth in the adhesive layer are: the elastic-brittle fracture energy $G_\mathrm{d}=1\times10^{-2}\mathrm{mJmm}^{-2}$, plastic slip yield stress $\sigma_{\mathrm{yield}}=0.56(2k_tG_\mathrm{d})^{-1/2}=5.3$MPa. The hardening slope for plastic slip is $k_\mathrm{H}=5\times10^2\mathrm{MPamm}^{-1}$. The energy due to gradient term should be small, so the auxiliary parameter k_0 is prescribed by a small number, $k_0=1\times10^{-3}$mJ.

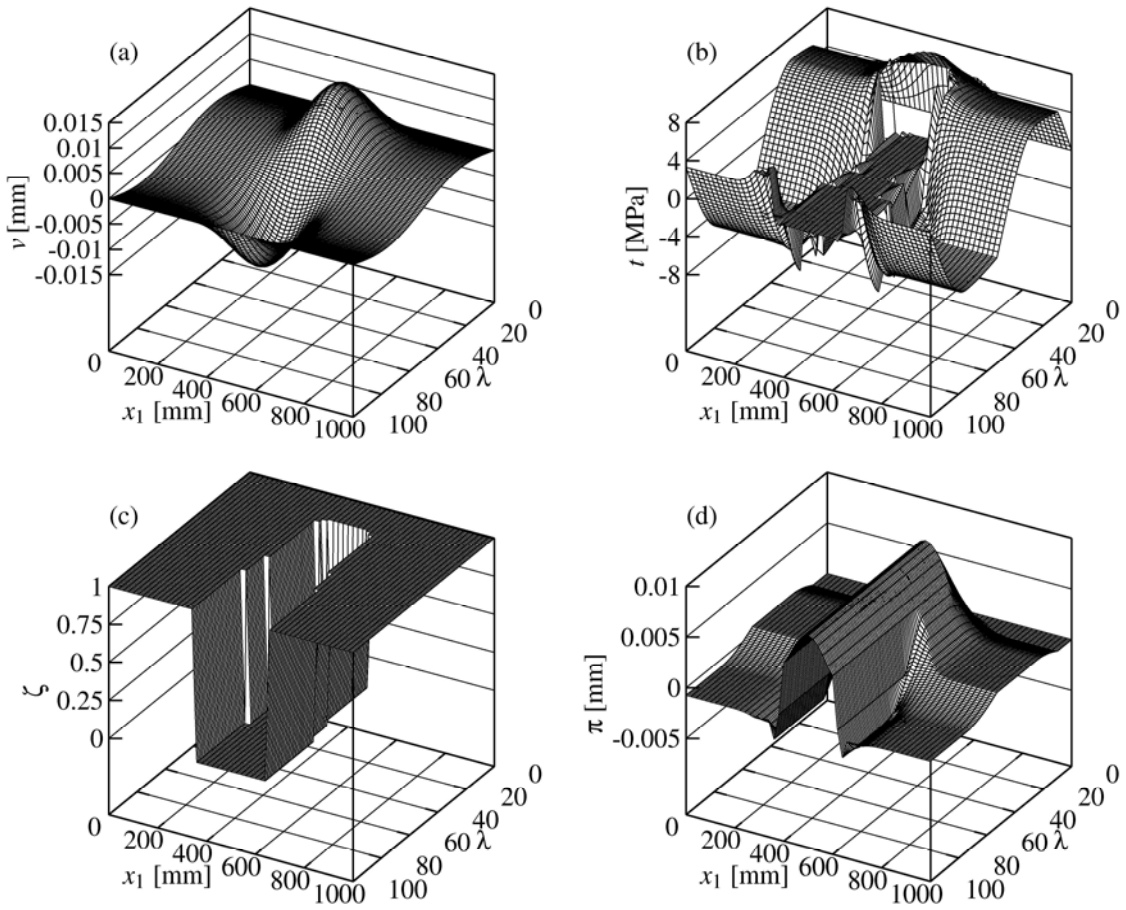

Figure 3: Distribution of the interface variables: (a) prescribed tangential displacement, (b) stress, (c) damage, (d) plastic slip.

The solution to the problem is shown in Figure 3. The prescribed displacement is drawn in the graph (a). The periodic loading changes both in magnitude and in direction. Naturally, due to the rupture of the interface, the periodic response of the structure is not expected. The initiation of the interface crack can be observed in all the graphs: the broken interface does not transfer stress in the graph (b), damage parameter ζ abruptly changes from one to zero in the graph (c) and the plastic deformation remains constant after the initiation of the crack in the graph (d). The parts of the interface with undamaged epoxy layer still hold the two rigid bulks together, though the layer is deformed plastically as it can be observed in the graph (d). It should be noted that the stress, which is not the variable of the solution process, is recovered after calculation by the relation $t=\zeta k_t(v-\pi)$.

The relations between the imposed displacement and the stress in the epoxy layer for two particular points are plotted in Figure 4.

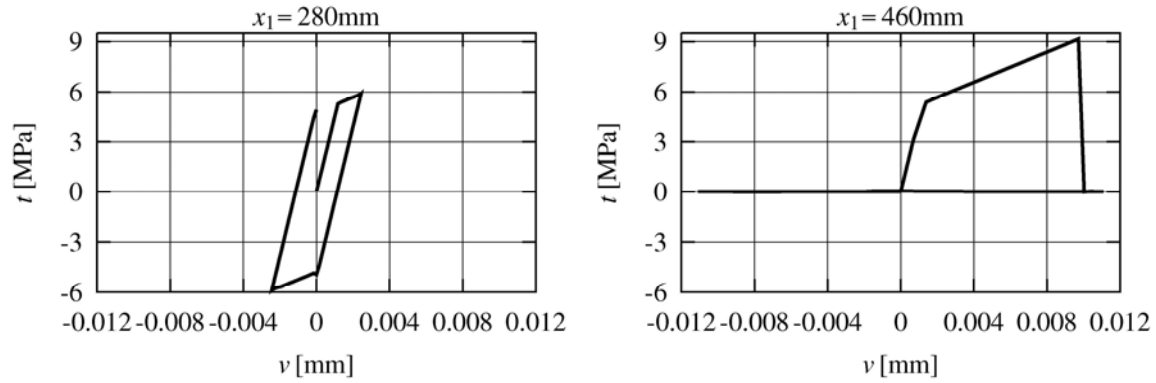

Figure 4: Stress-strain relation for two particular nodes.

The first point at x_1=280mm belongs to the unbroken part. The hysteresis related to the plastic deformation can be observed as the unloading obeys the elastic slope. The first plastic deformations appear exactly for yield stress σ_{yield}. The second point at x_1=460mm belongs to the part which breaks at the load step λ=18. This means that after initiation of plastic deformations the epoxy layer around this point deforms plastically until it is totally debonded from the bulk. Subsequent displacement loading does not have any effect in the relation as the layer remains stress free.

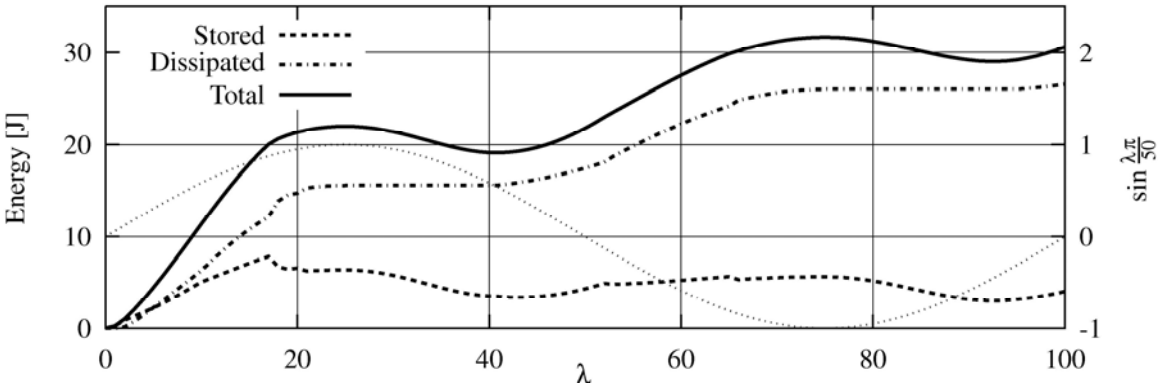

Figure 5: Energies in the process of crack initiation and growth.

Finally, an energetic evolution of the structure is presented in Figure 5. Three curves correspond to the energy stored in the epoxy layer (7), dissipated energy due to plastic deformation and rupture of the interface (2) and the sum of these two components. In order to understand the non-monotone behaviour of the total energy, a schematic drawing of loading and unloading process is included – the λ-dependent sin function of (11) is sketched by the dotted line. After achieving the maximum displacement, the upper bulk starts moving in the opposite direction which leads to consumption of the stored energy, also total energy is

decreasing. Nevertheless, the dissipated energy cannot be returned to the structure thus the pertinent curve is always non-decreasing. The energy plot also documents appearing of the plastic slip – at the point where the total and the stored energies separate – and crack initiation – at the point where the stored energy suddenly decreases.

5 Conclusion

An energy based model for initiation and growth of an interface crack under rate-independent conditions has been considered. The general model provides a kind of sensitivity to the mode of crack, i.e. whether the interface is broken in the opening mode, shearing mode or generally a combination of both modes. This sensitivity has been achieved by considering two internal variables along the interface: damage parameter ζ and plastic slip π.

The particular numerical analysis has been performed for an abstract example which resulted to the crack initiation and growth in shearing mode. The results confirm the expected behaviour of the proposed model and asses its applicability to problems with initiation and evolution of interface cracks.

Appendix: MATLAB routines

The solution of the example was obtained by a computer code written in MATLAB. Some parts of the codes, mainly concerning the optimization algorithms, are summarize in the following tables: the procedure of AMA in tab. Table 1, the procedure of BTA in Table 2 and an implementation of Polyak algorithm for bound constrained conjugate gradients in Table 3.

Table 1: Scheme of AMA (`MM, M, DM, m, m0` are matrices obtained by discretization of integrals in (2) and (7))

```
function [y,z] = fdpmline(v,y0,z0)
% [y,z] = fdpmline(v,y0,z0)
% Find minimum of E+R by alternation  for the prescribed v starting from pi0 and zeta0
% Input:  v  -- given slip
%         y0 -- initial plastic slip pi0
%         z0 -- initial damage state zeta0
% Output: y  -- plastic slip pi after applied displacement
%         z  -- final damage state zeta
%%%%%%%%%%%%%%%%%%%%%%%%%%%%%%%%%%%%%%%%%%%%%%%%%%%%
global kt kh k0 sy Gd MM M m m0 DM;
znew = z0;
z = zeros(size(z0));
% Alternation
while( max(z~=znew) == 1 )
  z = znew;
% Minimization with pi
  Asub = MMmult(MM,[],[],z);
  A = kh/4*[M -M; -M M] + kt/4*[Asub -Asub; -Asub Asub];
  bsub = MMmult(MM,[],v,z);
  b = kt/2*[-bsub bsub]-sy/2*[m m];
  omega = QP(A,b,[-y0 y0], inf,1e-6,size(A,1),[-y0 y0]);
  y = (-omega(1:end/2)+omega(end/2+1:end))*0.5;
% Minimization with zeta
  znew = QP(k0*DM,Gd*m0-kt/2*MMmult(MM,(v-y),(v-y),[]),0,z0,1e-6, size(DM,1),z0);
```

```
end
z = znew;
end
```

Table 2: Scheme of BTA (`LoadStep` calculates prescribed displacement v, `fdpline` evaluates energies from (2) and (7))

```
%Initiation
i=1; y0 = zeros(size(m)); z0 = ones(size(m0));
% Stepping in time
while(i=<(N+1))
  v(i,:)=LoadStep(i);
% Use alternation
  [x(i,:),z(i,:)]=fdpmline(v(i,:),x0,z0);
  if(i>1)
% Calculate energies
    [E(i), R(i)] = fdpline(v(i,:),x(i,:),z(i,:),x(i-1,:),z(i-1,:));
    Eup(i)=fdpline(v(i,:),x(i-1,:),z(i-1,:),x(i-1,:),z(i-1,:));
    Elow(i)=E(i)+E(i-1)-fdpline(v(i-1,:),x(i,:),z(i,:),x(i-1,:),z(i-1,:));
    DissR(i)=sum(R(2:i));
    T(i)=E(i)+DissR(i);
    z0 = z(i,:);
% Check possible back-tracking
    if((Elow(i)>E(i)+R(i)) || (Eup(i)<E(i)+R(i)))
      i=i-1;
    else
      i=i+1;
    end
  else
    z0 = z(i,:);
    i=i+1;
  end
  x0 = x(i-1,:);
end
```

Table 3: MATLAB implementation of Polyak algorithm (`BoxReducedG` calculates reduced gradient required for the algorithm, see [12])

```
function [x,n,relres] = QP(A,b,low,up,tol,maxit,x0)
% [x n relres]=QP(A,b,low,up,tol,maxit,x0)
% Polyak algorithm for minimization of 1/2xAx-bx with the bound up>=x>=low
% input:  A      - system SPD matrix
%         b      - system vector
%         low    - vector of lower bounds
%         up     - vector of upper bounds
%         tol    - required tolerance (relative residual)
%         maxit  - max. number of iterations
%         x0     - initial estimation
% output: x      - approximate solution within the given tolerance
%         n      - number of evaluated iterations
%         relres - relative residual of the approximate solution and all iterations
%%%%%%%%%%%%%%%%%%%%%%%%%%%%%%%%%%%%%%%%%%%%%%%%%%%%%%%%%%%%%%%%%%%%%%%%%%%%%%%%%%%
g =  A * x0 - b;
[gP,phi,beta]=BoxReducedG(g,x0,low,up);
p = gP;
n=0;
normr = norm(gP);
normr0 = normr;
relres(1)=1;
x=x0;
while ((normr>tol) && (n<=maxit))
    if(norm(phi)>tol)
        Ap = A * p;
        alphaCG = (g'*p)/(p'*Ap);
```

```
        y = x0 - alphaCG * p;
        testalphalow = (x0-low)./p;
        testalphaup = (x0-up)./p;
        alphaF = min([testalphalow(p>tol);testalphaup(p<-tol)]);
        if(numel(alphaF)==0 || alphaCG<=alphaF)
            x0 = y;
            g = g - alphaCG * Ap;
            [gP,phi,beta] = BoxReducedG(g,x0,low,up);
            bb = (phi'*Ap)/(p'*Ap);
            p = phi - bb*p;
        else
            x0 = x0 - alphaF * p;
            g = g - alphaF * Ap;
            [gP,phi,beta] = BoxReducedG(g,x0,low,up);
            p = phi;
        end
    else
        Abeta = A*beta;
        alphaCG = (g'*beta)/(beta'*Abeta);
        y = x0 - alphaCG*beta;
        testalphalow = (x0-up)./beta;
        testalphaup = (x0-low)./beta;
        alphaF = min([testalphalow(beta<-tol); testalphaup(beta>tol)]);
        if(alphaCG<=alphaF)
            x0 = y;
            g = g - alphaCG * Abeta;
            [gP,phi,beta] = BoxReducedG(g,x0,low,up);
            p = phi;
        else
            x0 = x0 - alphaF * beta;
            g = g - alphaF * Abeta;
            [gP,phi,beta] = BoxReducedG(g,x0,low,up);
            p = phi;
        end
    end
    normr = norm(gP)/normr0;
    n = n+1;
    relres(n+1,1)=normr;
end
if(n==(maxit+1))
    disp('Maximum number of iterations reached!')
end
x=x0;
```

Acknowledgements

The part of the work has been accomplished during the stage of the author at the University of Seville, supported by the Spanish Ministry of Education (Ref. SAB2010-0082). The author also acknowledges support from the grant VEGA 1/0201/11.

References

[1] GRIFFITH, A. (1921). The phenomena of rupture and flow in solids. *Philos. Trans. Royal Soc. London Ser. A. Math. Phys. Eng. Sci.,* 221, 163–198.

[2] BANKS-SILLS, L., ASHKENAZI, D. (2000). A note on fracture criteria for interface fracture. *Int. J. Fract.* 103, 177–188.

[3] HUTCHINSON, J.W., SUO, Z. (1992). Mixed mode cracking in layered materials. *Advances in Applied Mechanics,* 29, 63–191.

[4] LIECHTI, K., CHAI, Y. (1992) Asymmetric shielding in interfacial fracture under in-plane shear. *J. Appl. Mech.,* 59, 295–304.

[5] TVEEGARD, W., HUTCHINSON J. (1993). The influence of plasticity on mixed mode interface toughness. *Int. J. Physics of Solids.* 41, 1119–1135.

[6] TÁVARA, L., MANTIČ, V., GRACIANI, E., CANAS, J., PARÍS, F. (2010). Analysis of a crack in a thin adhesive layer between orthotropic materials: An application to composite interlaminar fracture toughness test. *CMES - Computer Modeling in Engineering and Sciences,* 58, 247–270.

[7] TÁVARA, L., MANTIČ, V., GRACIANI, E., PARÍS, F.(2011). BEM analysis of crack onset and propagation along fibre-matrix interface under transverse tension using a linear elastic-brittle interface model. *Engineering Analysis with Boundary Elements,* 35, 207–222.

[8] BESSON J., CAILLETAUD, G. CHABOCHE, J.L., FOREST, S. (2010). *Non-Linear Mechanics of Materials.* Dordrecht: Springer.

[9] ROUBÍČEK, T., KRUŽÍK, M., ZEMAN, J. (2012). Delamination and adhesive contact models and their mathematical analysis and numerical treatment. In V. Mantič, editor, *Mathematical Methods and Models in Composites*, Imperial College Press.

[10] ROUBÍČEK, T., MANTIČ, V., PANAGIOTOPOULOS, C. Quasi-static mixed-mode delamination model. *Discrete and Cont. Dynam. Syst.*, accepted.

[11] VODIČKA, R., MANTIČ, V. (2012). An SGBEM implementation of an energetic approach for mixed mode delamination. In: Advances in Boundary Element & Meshless Techniques XIII, 3.-5.9.2012, (319-324), Eastleigh, England: EC, Ltd.

[12] BOURDIN, B., FRANCFORT, A., MARIGO, J.J. (2008). *The Variational Approach to Fracture,* Berlin: Springer.

[13] ROUBÍČEK, T. (2004). *Nonlinear Partial Differential Equations with Applications.* Intl.Ser.Numer.Math 153. Basel: Birkhäuser.

[14] MIELKE, A., THEIL, F. (2004). Mathematical model for rate-independent phase transformations with hysteresis. *Nonl. Diff. Eqns. Appl.*, 11, 151–189.

[15] BOURDIN, B., FRANCFORT, A., MARIGO, J.J. (2000). Numerical experiments in revisited brittle fracture. *J. Mech. Phys. Solids*, 48, 797–826.

[16] DOSTÁL, Z. (2009) *Optimal Quadratic Programming Algorithms*, *Springer Optimization and Its Applications,* 23. Berlin: Springer.

[17] BAŽANT, Z., JIRÁSEK, M. (2002) Nonlocal integral formulations of plasticity and damage: Survey of progress. *J. Engrg. Mech.*, 128(11), 1119–1149.

[18] MATLAB (2009). V 7.9.0.529. The MathWorks, Inc.

[19] BARTELS, S., KRUŽÍK, M. (2011). An efficient approach to the numerical solution of rate-independent problems with non-convex energies. *Multiscale Model. Simul.* 9(3), 1276–1300.

[20] TÁVARA, L., MANTIČ, V., GRACIANI, E., PARÍS, F. (2011). BEM analysis of crack onset and propagation along fibre-matrix interface under transverse tension using a linear elastic-brittle interface model. *Eng. Anal. Bound. Elem.*, 35, 207–222.